Indian Geotech J (March 2018) 48(1):52–71
https://doi.org/10.1007/s40098-017-0229-7

ORIGINAL PAPER

Testing and Modelling of Screw Nailed Soil Slopes

Saurabh Rawat[1] · Ashok Kumar Gupta[1]

Received: 25 November 2016 / Accepted: 20 February 2017 / Published online: 24 February 2017

Abstract This paper aims at testing and numerical modelling of soil slopes reinforced by using screw nails. Two model soil slopes at 45° and 90° with the horizontal are stabilized by inclusion of six screw nails at 0° inclination with horizontal. The screw nailed soil slopes are subjected to an increasing surcharge load at slope crest and their failure mechanism is studied. The present investigation also examines the failure load and displacement, failure surface and volumetric deformation of screw nailed slopes. Numerical modelling of the two screw nailed slopes using limit equilibrium method and generalized finite element analysis method has also been carried out. Factor of safety along with failure slip surfaces has been analysed by limit equilibrium method. Generalized finite element analysis is used with strength reduction method to determine factor of safety and slip surfaces. The slope displacement, failure load and volumetric deformation of these two screw nailed slopes are also studied by generalized finite element analysis method. The model testing results are validated by its numerical modelling. It is found that factor of safety, slip surfaces, load–displacements from testing and modelling are in accordance with slight variations. A comparative study between factor of safety and load–displacement of slopes with smooth nails and screw nails under study is also done. A higher factor of safety and a decrease in slope displacement is observed for screw nailed slopes. With the advantage of ease of installation, the screw nails are found to provide sufficient slope stability for the two modelled slopes.

Keywords Testing · Modelling · Screw nail · Slope stability · Failure mechanism

✉ Ashok Kumar Gupta
ashok.gupta@juit.ac.in

1 Department of Civil Engineering, Jaypee University of Information Technology, Waknaghat, Solan, Himachal Pradesh 173234, India

Introduction

The conventional process of soil nailing simply comprises of inserting reinforcing inclusions (nail), which is typically in the form of reinforcement steel bar that is placed at an angle below horizontal in a drilled borehole and subsequently encased in cement grout. One of the many drawbacks of the conventional soil nail system is that its performance is very much dependent on pullout resistance of nail. The pullout resistance of nail in turn depends on type of soil, soil moisture content, soil dilation, nail type, nail properties such as surface roughness, nail bending, installation processes, overburden pressure and grout pressure [1, 2]. Other shortcoming of conventional soil nail is the problem of 'bridging' [3]. As a result of actual drilling process, the surrounding soil stresses are altered which allows mobilization of only a limiting value of nail pullout resistance and also renders it independent of surcharge pressure. The structural integrity of nail and its compressive strength is also compromised, if at grouting stage, the grout is allowed to flow under gravity at low pressures to fill the voids. During the installation of nails, a poorly centralised bar can reduce the bending strength of nail. It can also lead to cracking of grout and subsequent breakage of nail. Another installation difficulty with a grouted soil nail is its construction complexities in soils like silt, sand, gravel and cobbles [4], where a tendency of high ground loss due to drilling technique is observed for course grained soil [5].

Apart from installation limitations, the soil-tension element friction is one of the basic factors influencing the deformation and strength of reinforced soils [6]. The load transfer from soil to nail is through the mobilized friction at the soil–nail interface [7]. For better understanding of this apparent coefficient of friction between nail–soil and nail pullout resistance has been studied experimentally and analytically by several researchers [8–15]. Chu and Yin [16] conducted a comparative study between shear strength from direct shear and pull out testing which concluded that the angle of interface friction can be improved by increasing the interface roughness angle.

An approximate estimate of the response of actual field soil nailed slopes can be done by laboratory model testing on a similar prototype. The failure mechanism of reinforced slopes under surcharge loading along with other parameters like slope deformation, optimum nail inclination, nail forces and slope load carrying capacity has been studied by model testing [17–21]. In addition to experimental simulation, numerical modelling of nailed soil slopes is carried out using Limit equilibrium method (LEM), Finite element method (FEM) and Finite difference method (FDM) also. However, FEM has always been considered to predict much realistic results which are in good agreement to the in-situ soil nailed slope or cut response [22–25].

From the literature review, it can be concluded that the installation problems related to conventional nails can be overcome, if a nail is developed which can be installed without grouting. This will not only minimize the disturbance to the adjacent soil, but also produce fewer spoils [26]. Moreover such nails can also be effectively employed in ground conditions with coarse grained soil like silt and sand. Moreover, if such a nail has a rougher surface than conventional smooth surface nail, then it will be able to mobilize a greater apparent interface friction. This will further enhance its reinforcing potential in slope stabilization. In order to achieve this, an innovative screw nail has been used in the present study. The behaviour of screw nailed soil slopes at two different slope angles (β) of 45° and 90° with horizontal are studied by conducting small scale model tests. These new screw nails are installed at a nail inclination (θ) of 0° with horizontal for all slope angles. The stabilizing effect of screw soil nailed slopes is studied by determination of factor of safety for both nailed slopes by LEM using a software package Slope/W. Finite element modelling of screw nailed slopes of 45° and 90° is also carried out by a finite element (FE) code, Plaxis 2D for understanding load–deformation characteristics, volumetric deformations, potential slip surfaces generated and factor of safety for reinforced slopes under study. The results of model testing are validated by its numerical modelling both by LEM and FEM sub-routines. Moreover, a comparative study between smooth nailed soil slopes from literature and screw nailed soil slopes of present study has been done to bring out the difference in their reinforcing contributions to unstable slopes.

Testing Procedure

Development of Screw Nail

The screw nail used in the present work has been developed using mild steel solid bar having a diameter of 16 mm. The steel bar is worked upon by a thread rolling machine which renders its surface with threads of height 0.15 mm. Thus, the fabricated screw nail has major diameter (D) of 16 mm and minor diameter of 15.7 mm. The end of screw nail, about 20 mm in length is made tapered to ease the initial penetration in soil slope. The effective screw nail length used is 150 mm from nail head. The total nail length taken for model testing is 170 mm for slope height of 30 cm. Bruce and Jewel [27] suggested that for slopes with granular soils, the length ratio i.e. ratio of maximum nail length to excavation height for drilled and grouted soil is between 0.5 to 0.8 and 0.5 to 0.6 for driven nails. Gosavi [28] also states that the commonly used length of nail (L)/height of cut (H) ratio are in the range of 0.5–0.8. Using length ratio of 0.56, the nail length has been adopted as 170 mm. Moreover, smaller length ratios of 0.28, 0.21 and 0.14 have also been used by Zhang et al. [29] for model testing of reinforced slopes. Plumelle and Schlosser [30] and Byrne et al. [31] observed that the location of the failure surface is controlled by global limit equilibrium considerations. Strain measurements in instrumented soil nailed walls have indicated that in the upper portion of the wall, the maximum tensile force occurs approximately between 0.3 and 0.4 H behind the wall facing, while in the lower portion of the wall, the maximum tensile force occurs approximately between 0.15 and 0.2 H behind the wall facing. This signifies that the failure surface can be expected to intersect the nail length of 0.56 H. It has also been observed by Fan and Luo [24] that nail length on the upper 1/3 height of slope and middle 1/3 of slope height has minor influence on the factor of safety, which is governed mainly by tensile stresses mobilized in nails. However, nail length in lower 1/3 of slope height contributes significantly to stability of soil nailed slopes. This behaviour can be explained by the following reasons: (1) nails located at the lower level of slopes bear greater overburden stresses than those located at the upper part of slopes. Thus, greater pull-out resistance is expected for nails at the lower part of slopes compared to those at the upper level of slopes and (2) nails located at the lower part of slopes tend to develop more tensile forces than those located at the upper part of slopes and tensile forces in nails is more effective in mobilizing shear resistance against shear deformation in soil mass. Hence, nails located at the lower part of slopes may provide more shear resistance against shear deformation in soil mass. Based on the above reasons it is recommended to have nail length of at least 1.0× the height of slopes at lower 1/3 part to ensure effectiveness of nail action on the overall stability of slopes. In the present work, nail length of 1.5 times the height of slopes at lower 1/3 part has been used to stabilize the slopes. An arrangement of a small handle is provided at the nail head to facilitate the rotation of screw nail during installation. This arrangement will also serve as a nail head which is fixed on the slope facing. The screw nail used in the present work is shown in Fig. 1. The properties of screw nail are determined by conducting tensile test on a sample screw nail in Universal testing machine. The modulus of elasticity of screw nail (E_{sn}) as obtained from stress–strain plot is 200 GPa and Poisson's ratio of screw nail (υ_{sn}) is 0.3.

Fabrication of Model Tank and Soil Slopes

A rectangular 60 cm (length) × 40 (width) cm × 60 (height) cm model tank is fabricated using Perspex sheets of thickness 12 mm. The Perspex sheets are fastened to the iron angles by bolts. The sides of the tank are braced by iron strips to restrain the lateral deformation of sheets during testing. The tank was filled with sand obtained locally for construction of slopes at desired slope angles. The construction of soil slopes is carried out by rainfall technique to attain a specified unit weight (γ) = 16.5 kN/m^3 for both the slopes. This unit weight corresponds to a relative density of 70% [19]. The mass of soil used for construction of 45° and 90° slopes is 152 and 120 kg respectively. A similar process of slope construction has also been done by Gosavi et al. [32]. The specific gravity of fill material is determined from pyconometer test, sieve analysis was carried out to determine the soil type and shear strength parameters were determined from direct shear test. From these tests, it was concluded that the soil used in slope construction is a poorly graded sand soil (SP) with specific gravity of 2.68. A moisture content of 18% is added to poorly graded sand in order to facilitate the construction of 45° and 90° slopes. The moisture content of 18% is optimum moisture content obtained from proctor test which corresponds to a maximum dry unit weight of 13.98 kN/m^3. The shear strength parameters of fill material are determined by Direct shear tests under consolidated drained (CD) conditions with 18% moisture content, which yields a cohesion value of 10.41 kN/m^2 and angle of internal friction as 30.79°. All the parameters of fill material are given in Table 1.

The step-wise procedure for both slope constructions of 45° and 90° is as follows: (1) A temporary plywood slope facing is fixed at the desired inclination inside the model tank. To ensure correct slope inclination, markings are made on the perspex sheet. (2) With the plywood facing intact, the sand is filled in model tank with rainfall technique. The first layer is the base layer with a height of 10 cm. (3) At regular intervals, red colour dye tracer powder is used. It enables the observer to physically study deformation of soil layers during loading by its altered pattern. (4) Above the base layer with tracer, next soil layer is constructed as mentioned above. (5) The process is repeated till the desired height of 30 cm of slope is achieved. (6) The finished slope with model box is weighed. Since unit weight and mass is known, the volume of soil used in construction of slopes is calculated.

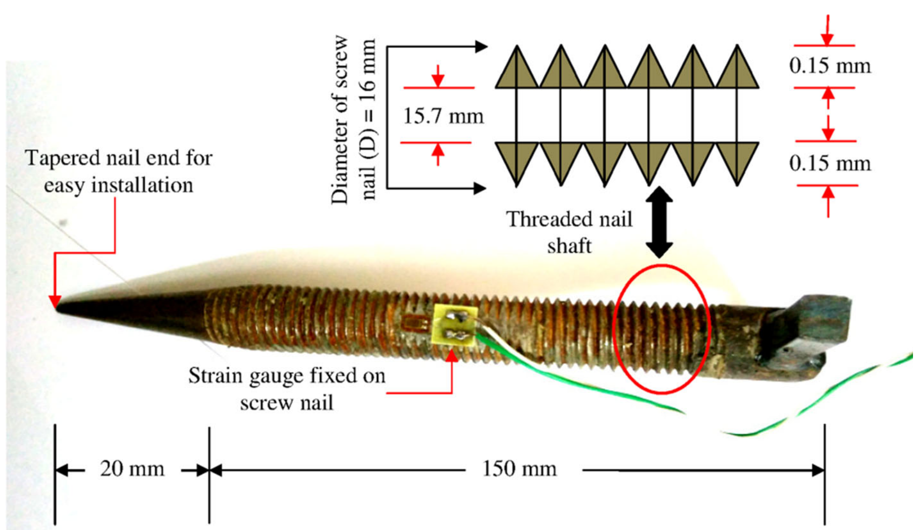

Fig. 1 Details of screw nail used

Table 1 Properties of fill material

Properties	Values (units)
Specific gravity (G)	2.68
Soil type	Poorly graded sand (SP)
Moisture content (w)	18%
Cohesion (c)	10.41 kN/m^2
Angle of internal friction (ϕ)	30.79°
Maximum dry unit weight (γ_d)	13.98 kN/m^3
Initial void ratio (e_0)	0.88

Determination of Screw Nail-Soil Interface Friction

Direct shear tests (DST) are conducted with soil–soil (without nail) and soil–soil (with nail) conditions in standard Direct shear box with plan area of 6 cm × 6 cm and sample depth of 5.3 cm to study the interface friction between screw nail and soil. A screw nail sample of circular cross-section having a minor diameter of 15.7 mm with threads of height 0.15 mm along a nail length of 40 mm is placed symmetrical in both plan and elevation [33] in the direct shear box as shown in Fig. 2. The sample screw nail used in DST has modulus of elasticity (E_{sn}) of 200 GPa and Poisson's ratio (υ_{sn}) of 0.3, which are similar to those used in model tests. From Fig. 3, it can be clearly seen that an increase in coefficient of friction and cohesion is observed as surface roughness increases between soil–soil interface due to the presence of a screw nail. Chu and Yin [16] states that "The shear failure envelope for the irregular surface of soil nails is mostly above the shear failure envelope for the regular surface of soil nails, and the slope of the failure envelope is increased as the soil–grout (i.e. grout and soil surrounding the grout) interface surface roughness increases. The peak interface friction angle can be higher than the soil friction angle for irregular surface nails." The surface roughness of screw nails can thus be accounted for producing a better sliding friction than conventional smooth surface nails.

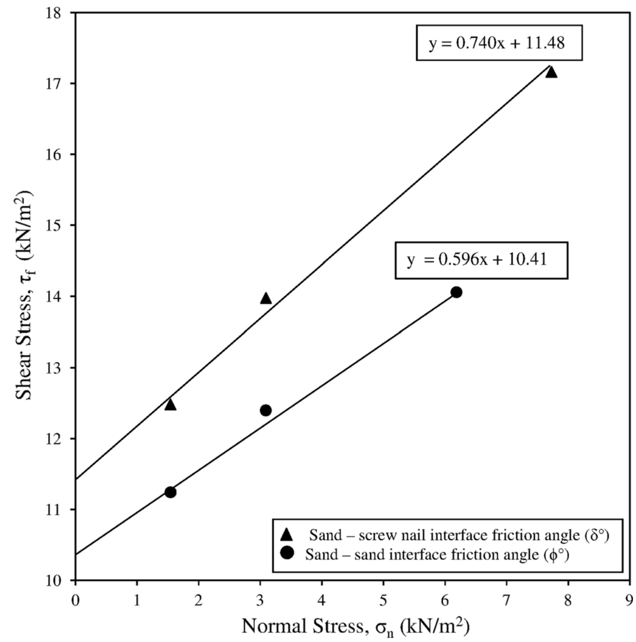

Fig. 3 Shear failure envelop from direct shear tests

The soil–nail interface is higher than soil friction angle because when screw nail is embedded in sand during direct shear test with nail condition, soil is displaced. This soil

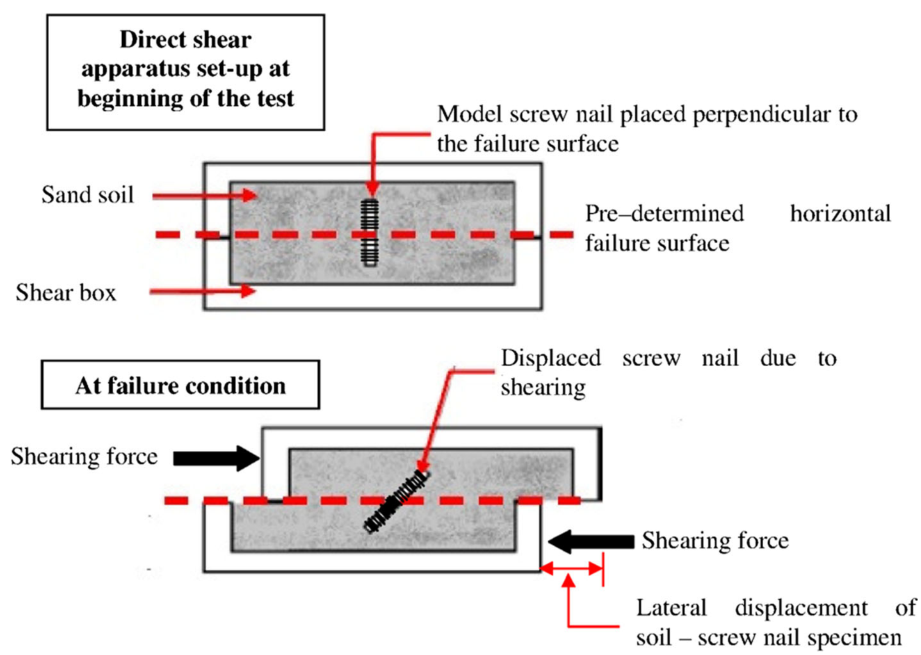

Fig. 2 Set-up of direct shear test with screw nail

Table 2 Shear parameters from direct shear tests

Interface	Angle of internal friction	Interface friction coefficient	Cohesion (c) in kN/m^2
Sand–sand	$\phi = 30.79°$	tan ($\phi°$) = 0.596	10.41
Sand–screw nail	$\delta = 36.5°$	tan ($\delta°$) = 0.740	11.48

displacement and soil enclosed between threads of screw nail leads to further densification of soil around the screw nail which causes an increase in normal stress along nail length. This change in stresses around screw nail moves the failure surface away from the soil–nail interface. The weak planes are found to lie within the thin densified soil zone created around the screw nail. The shear failure of soil–nail interface is now governed by this interface between the newly dense soil zone. As the friction angle of soil has increased in this zone compared to the surrounding soil, higher soil–nail interface friction angle is observed. However, pullout test on screw nail can further enhance the understanding of the increase in interfacial friction and cohesion. The results of direct shear tests are summarized in Table 2.

The cohesion value obtained is attributed to moisture content added in sand to facilitate model slope preparation. This moisture content induces 'apparent cohesion' in between the soil particles which is reflected by obtaining a value of 'c' for sand. The difference between values of 'c' for sand–sand and sand–screw nail is also quite less because introduction of screw nail in sand only influences interface roughness and not the induced apparent cohesion. However, a slight increase in 'c' value between with and without nail condition can be accounted for soil densification due to displacement of soil when the nail is embedded in the soil sample.

In the absence of pullout results for screw nails, the coefficient of friction for pullout test (f*) is determined by the coefficient of friction from direct shear test (f). The relation between the two coefficients is given by Wang and Richwein [6].

$$f^* = \frac{f}{1 - \left\{\frac{2(1-\upsilon)}{(1-2\upsilon)(1+2K_0)}\right\}(f \tan\psi)} \quad (1)$$

where, υ = Poisson's ratio of soil taken as 0.33; K_0 = Earth pressure coefficient at rest which is calculated by the Jaky's formula as ($1-\sin\phi$); ψ = Dilation angle of soil calculated by ($\phi°-30°$). Using Eq. (1), the coefficient of friction from pullout for screw soil nail is calculated as $f^* = 0.766$. It can be seen that 'f*' is slightly greater than 'f' for sand–screw nail interface, which is in agreement to the observation made by Kulhawy and Peterson [34] stated as "The interface friction angle δ' is less than the soil friction angle ϕ' for smooth interfaces, and the interface friction angle δ' is equal to or greater than the soil friction angle ϕ' for rough interfaces.

Installation of Screw Nails in Slopes

As shown in Fig. 1, the screw nails are provided with an arrangement at nail head. The nails are screwed—in through the holes in slope facing. The holes are located at specified distances with equal horizontal spacing of 13.3 cm from edge of facing for both slope angles of 45° and 90°. The vertical spacing of 10.5 cm between the holes for 45° is calculated from the slanting height of slope of 42.42 cm. For 90° slope, vertical spacing between the holes is maintained at 7.5 cm for slope height of 30 cm. The nails are arranged in rectangular pattern with equal horizontal spacing and different vertical spacing corresponding to slanting height of slopes. A total of six screw nails are installed in a pattern of three rows and two columns. Moreover, the influence area for each nail i.e. $S_h \times S_v$ should be less than or equal to 4 m^2 as recommended by FHWA [35]. In the present work, the influence area of nails in 45° and 90° are well within the governing condition. The rectangular soil nail pattern as adopted for the present study facilitates easier construction of vertical joints in shotcrete facing and continuous installation of drain pipes behind the facing in field. It is also treated as the most commonly used soil nail pattern along with square pattern [35]. The screw nails are also provided with a tapered end which further facilitates easy nail installation without causing much disturbance to soil and producing no spoils. The inclination of screw nails is kept at 0° from the horizontal for both slope angles. At the centre of nail length, a strain gauge is fixed to measure the strains produced during slope loading. The completed screw nailed slope is shown in Fig. 4.

Model Testing

The modelled screw nail soil slopes are tested for slope-deformation failure by applying an increasing surcharge load at the slope crest. To ensure uniform distribution of load on slope crest, a steel plate with a plan area of 20 cm × 40 cm and thickness 4 mm is placed on the slope crest. The thickness of iron plate for uniform distribution on slope crest is selected after repeated trials with iron

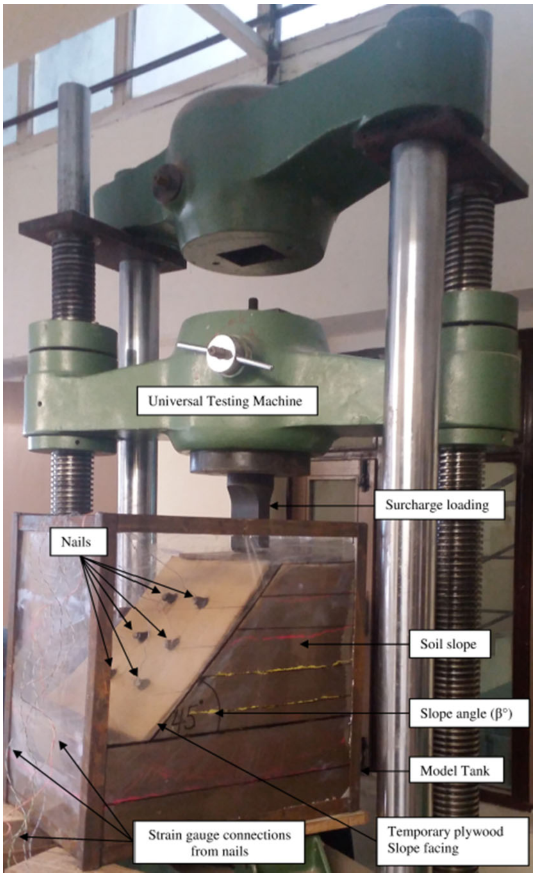

Fig. 4 Screw nailed soil slope test set-up

plates of thickness 2 and 3 mm. Both iron plates of thickness 2 and 3 mm are found to be thin leading to bending under the point of application of load from UTM and thus leading to non-uniform pressure distribution. However, using a 4 mm thick iron plate, no such bending and plate deformation is found during load application on slope crest. Thus, uniform distribution of load on slope crest was ensured.

The load is applied on 20 cm × 40 cm crest plan area. The plunger of the Universal Testing Machine (UTM) is placed at centre of iron plate to apply the surcharge loading. The UTM is attached to a digital meter which gives the load and settlement values on the slope. The strains generated along the nails during loading are measured by strain gauges attached and read off from the multimeter connected to each nail.

Results from Model Testing

The slope deformation, crest settlement and failure mechanism are determined from model testing on screw nailed slope.

Failure of Screw Nailed Soil Slopes

From Fig. 5a, b, it can be observed that as the slope is subjected to surcharge loading, the 45° reinforced slope undergoes deformation. This is evident from the settlement C_1, C_2 and C_3 and slope deformation D_1, D_2 and D_3 as marked in Fig. 5b. Before the surcharge load is applied on the slope, the slope face is flush with the marked undeformed slope face. As the surcharge loading increases, the shear strength of soil is mobilized. As the mobilized shear strength reaches it limiting value, soil movement takes places which causes the deformation of slopes. Once the shear strength of reinforced soil exceeds it limiting value, a slip surface generates. The slip surface generates at the crest of slope and propagates towards slope face. For a 45° reinforced slope, the potential slip surface starts at the slope crest and terminates at the slope face above the toe. In addition to this slip surface, small local cracks are also observed during testing. These local cracks mark the other weaker zones of the slope.

Figure 5b also suggests that surcharge also makes the slope settle along with longitudinal movement of slope. This can be visualized from final level reached by the tracer marking along the slope height. This soil movement is also important with the view that a soil nailing system is a strain compatibility problem. A certain amount of strain or soil movement is required in order to stimulate the reinforcing action of screw nails.

A similar deformation pattern is observed for reinforced soil slope model of 90°. The undeformed 90° vertical slope or cut is shown in Fig. 6a, which corresponds to the stage when no surcharge is applied to slope crest. With the increase in surcharge loading, the 90° slope with screw nails undergoes deformation marked by as C'_1, C'_2 and C'_3 along the slope height and D'_1, D'_2 and D'_3 along the slope length. The settlement of slope crest and the slope body can be observed by the change in tracer level from initial level. The slope face deformation in the horizontal direction can be investigated from the soil mass movement beyond the undeformed slope face marking as shown in Fig. 6b. The slip surface at failure is found to generate from slope crest but much near to slope face as compared to that in 45° reinforced slope. Moreover, large horizontal deformations are observed at the slope crest with respect to that at toe. During testing it is observed that as the load increases, the 90° screw nailed slope initially rotates about its toe and then moves outwards. Similar to 45° screw nailed slope, this slope also develops local cracks at other locations within the slope which signify soil failure of weaker zones. This movement of soil under loading leads to mobilization of interface shear force between screw nail and soil, which makes the nails participate in load transfer mechanism of soil–screw nail system.

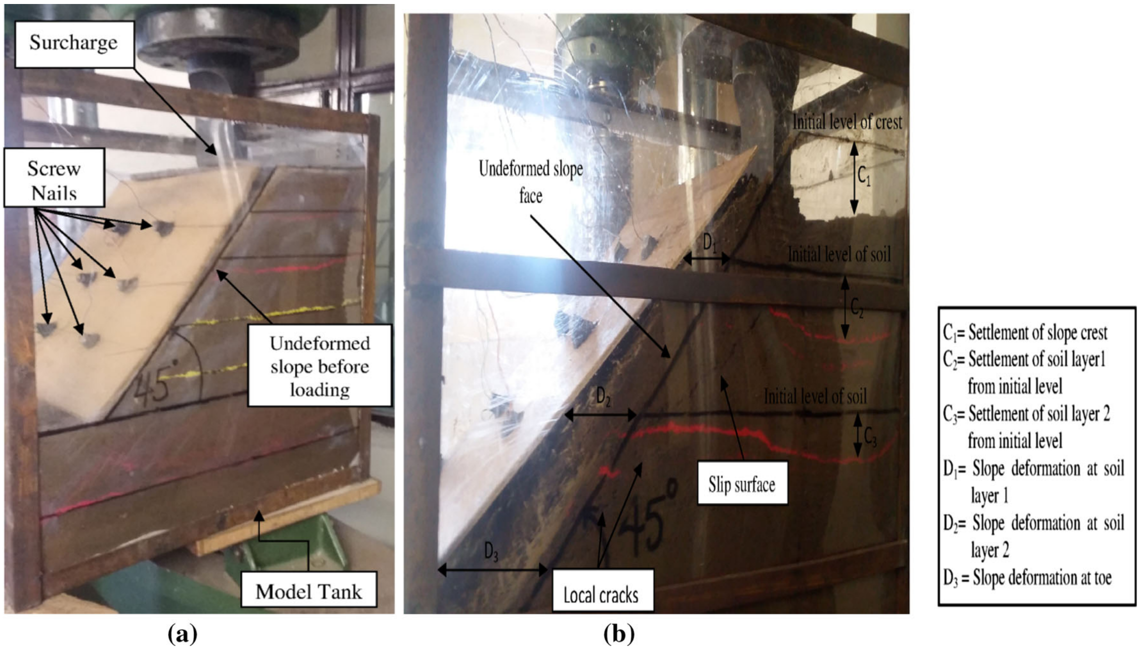

Fig. 5 45° screw nailed soil slope **a** before testing **b** after testing

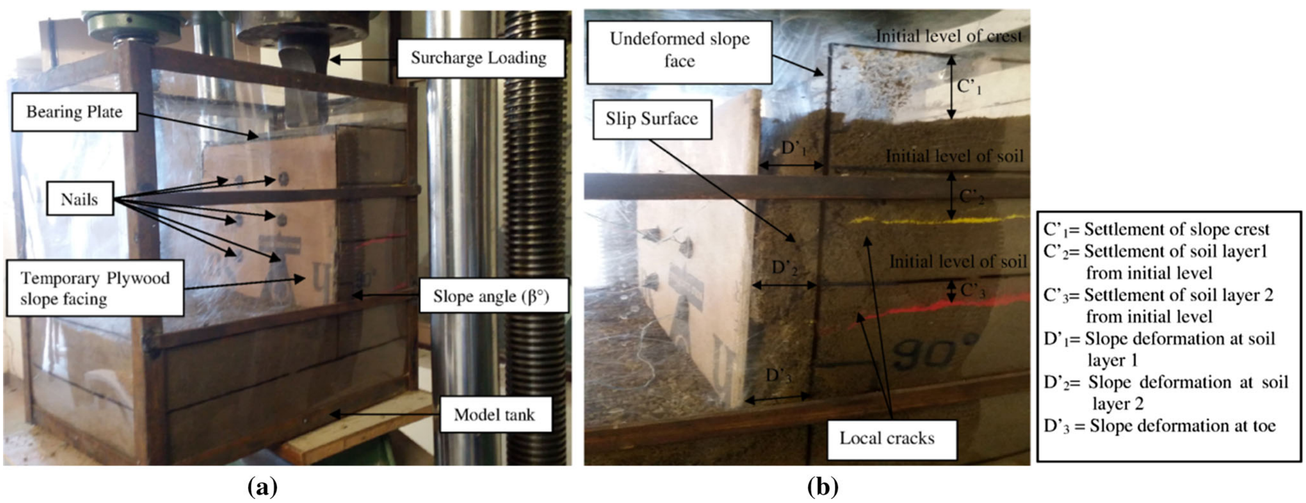

Fig. 6 90° screw nailed soil slope **a** before testing **b** after testing

Load-Settlement of Screw Nailed Soil Slopes

Table 3 gives the failure load and corresponding settlement for 45° and 90° slopes. It is found that 45° screw nailed slope shows failure at load of 41 kN with a slope settlement of 125 mm measured at slope crest. However a smaller load carrying capacity is found for 90° screw nailed slope which undergoes a settlement of 71.98 mm at a failure load of 30.20 kN.

The settlement of slope crest is due to soil compression under loading. The reinforced slope initially bears the load which causes densification of soil mass. As surcharge load increases, it is transferred to the nails along with soil overburden. As the crest starts to fail in bearing, cracks are generated at the crest. This initiates the failure surface. As the crack develops progressively, movement of slope occurs in horizontal direction along the slope length. This soil movement develops strains in reinforced soil slope. Due to these strains, the shear stresses are developed at soil–screw nail interface. Moreover, with increase in normal stress due to surcharge and overburden, additional stabilizing shear forces are also developed around screw nails. Since interface friction is greater than angle of internal friction of soil, the developed shear forces are also

Table 3 Load–settlement results from model testing

Slope with screw nail at 0° with horizontal	Failure load (kN)	Settlement (mm)
45°	41	125
90°	30.20	71.98

increased. This increase the bearing capacity of reinforced slopes and decreases the soil movement. Another reason for settlement of slope crest could be due to shearing of soil mass which causes an outward movement of slope.

Volumetric Deformation of Screw Nailed Slopes

As the loading of reinforced slopes is carried out, it is observed that both slopes have undergone volumetric deformation. In order to study this parameter, the model box are marked with 5 cm grids to quantify the amount of soil that has collapsed due to slope failure. From Fig. 7a, it is investigated that the amount of collapsed soil at crest and residual soil at slope face are not equal. The amount of soil collapsed is about 10,000 cm^3, whereas the residual soil amounts to 4000 cm^3 only. This can be calculated by observing the number of grids corresponding to change in slope height (ΔH) and change in slope length (ΔL) through the grid pattern. This further signifies that under loading condition the reinforced slope has not only deformed from original state but has also undergone compression.

From Fig. 7b, volumetric deformation for 90° slope can be estimated by a similar calculation using 5 cm grid pattern. The collapsed soil amounts to 4000 cm^3 in comparison to the amount of residual soil of 2500 cm^3. This unequal amount of collapsed and residual soil also signifies densification of slope soil under surcharge loading.

The results of volumetric deformation as studied through grid method are summarized in Table 4. A dimensionless parameter, Volumetric deformation index (V_D) defined as the ratio of change in slope volume (ΔV) to original slope volume (V) has also been derived.

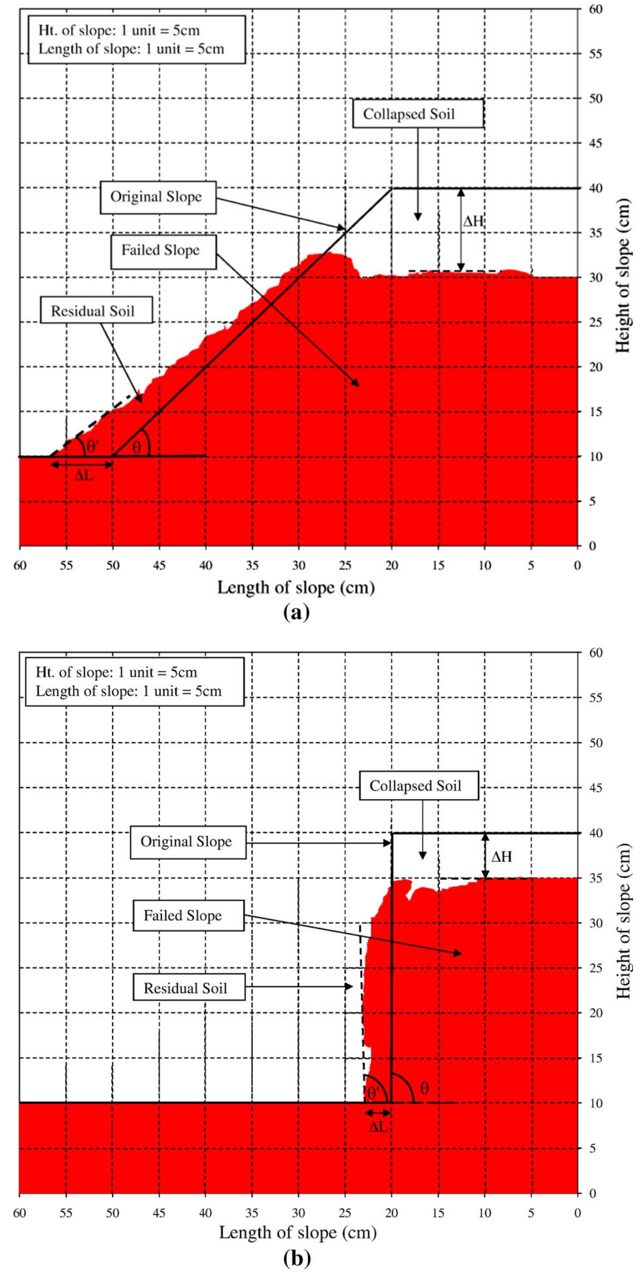

Fig. 7 **a** Volumetric deformation of 45° screw nailed soil slope. **b** Volumetric deformation of 90° screw nailed soil slope

Numerical Modelling of Screw Nailed Soil Slopes

The numerical modelling of screw nailed soil slopes is carried out using limit equilibrium method (Slope/W) and generalized finite element method (Plaxis 2D) software packages. In the present study, modelling in Slope/W is carried out to find the factor of safety for most critical slip surface. Numerical modelling in Plaxis 2D is used to study the load–deformation characteristics and volumetric deformations of screw nailed slopes. Factor of safety corresponding to failure surface is also calculated by Plaxis 2D.

Modelling with Slope/W

The Slope/W sub-routine employs LEM to calculate the factor of safety for the most critical slip surface. The input parameters required for modelling soil are unit weight of soil, soil cohesion and the angle of internal friction. All these values are taken from Table 1. The dimensions of soil slope are same as that used in model testing converted to scale. The most important feature of this modelling technique is simulation of screw nails. Slope/W does not provide the option of modelling the interface element between

Table 4 Volumetric deformation of screw nailed slopes using 5 cm grid

Reinforced slope angle	Original volume (V) in cm^3	Width of slope (cm)	Area of collapsed soil (cm^2) using 5 cm grids	Volume change (ΔV) in cm^3	Volumetric deformation index ($V_D = \frac{\Delta V}{V}$)
45°	90,278.78	40	250	10,000	0.110
90°	71,345.45	40	100	4000	0.056

nail surface and soil. The soil nail reduces the activating driving forces and increases the shearing resistance. This leads to an increase in stability of slopes. In SLOPE/W soil nails are treated as concentrated loads which reduce the destabilizing forces in soil slopes [36]. Screw soil nails are simulated in terms of pullout load which is calculated theoretically by using the coefficient of friction for pullout test (f^*) in equation from Gosavi et al. [7] for smooth nails as given in Eq. 2. Using this pullout load which incorporates the roughness in terms of interface friction of screw nails, pullout resistance is determined by Eq. 3 as given by Tokhi [3]. Thus, screw nails with its surface roughness are modelled into SLOPE/W. In addition to this, the input parameters required to simulate nails in Slope/W are tensile capacity and shear force of nails. All these input values are factored by a reduction factor. The reduction factor is defined as the reduction of the ultimately tensile capacity due to physical processes such as installation damage, creep and durability. It is applied to the strength of the nail to account for uncertainties in structure geometry, soil properties, external applied loads, the potential for local overstress due to load non-uniformities and uncertainties in the long-term nail strength. The value of reduction factor (RF) = 0.65 used in the present work has been adopted in accordance to Soil Screw Design Manual by Hubble [37].

$$Pullout\ load(P) = f^* \times \pi dL(\gamma z + q) \tag{2}$$

$$Pullout\ resistance(\tau_{max}) = \frac{P}{\pi dl} \tag{3}$$

Substituting Eq. (2) in Eq. (3), with $f^* = 0.766$ for screw nails as calculated in Sect. 2.2, depth of nails from slope crest (z) of 45° as 7.42, 14.85, 22.27 m for Screw nail 1, Screw nail 2 and Screw nail 3 respectively, unit weight of soil (γ) as 16.5 kN/m^3 and a surcharge (q) of 512.5 kN/m^2, the pullout resistance is determined. Similarly, for 90° slope, screw nails are simulated by taking $f^* = 0.766$, $z = 7.5$, 15 and 22.5 m respectively, $\gamma = 16.5$ kN/m^3 and $q = 377.5$ kN/m^2. The pullout resistance as calculated for each nail is given in Table 5.

The tensile capacity (T_a) and shear force (V) for screw nails is calculated from equation given by Hubble [37].

$$T_a = A_c(RF)f_y \tag{4}$$

where, A_c = cross-sectional area of screw nails (m^2); f_y = Yield strength of screw nails taken as 250 MPa; RF = Reduction factor of 0.65

Table 5 Pullout resistance calculated for each screw nail for Slope/W

	Screw nail 1 (kN)	Screw nail 2 (kN)	Screw nail 3 (kN)
45°	486.36	580.26	674.05
90°	383.96	478.75	573.54

$$V = 2A_b(RF)F_v \tag{5}$$

where, A_b = cross-sectional area of bolt (m^2); ultimate shear stress of steel (F_v) = $0.5E_{steel}$; E_{steel} = 200 GPa.

Using the above equations, the screw nail parameters are modelled for slope of 45° and 90°. The completed 90° screw nailed slope is shown in Fig. 8. The reinforced slopes are then analysed using Morgenstern-price method to find critical slip surface and determine factor of safety from moment equilibrium and force equilibrium.

Modelling with Plaxis 2D

Plaxis 2D is a FE code in which the continuum is divided into distinct elements, with each element further divided into nodes. Each node is assigned a degree of freedom depending upon the set of boundary conditions defined. The degrees of freedom of nodes are related to its displacement values. Each line element in the continuum is divided into 3 nodes which are used to build up 6 noded triangles. Similarly, if the line element has 5 nodes, a 15-noded triangle is generated. Since 15- noded triangles are found to yield more accurate results as compared to 6-noded triangles [38], the reinforced soil slopes are modelled as 15-noded triangular elements. The dimensions of numerical model of soil slope are similar to Slope/W model. To simulate the boundary condition similar to model testing, standard fixities are used. The model base is restricted in both x and y directions. The soil slope is set to free deformation in y-direction along its height and at a distance of 60 cm from slope back. The use of Mohr–Coulomb constitutive model simulates a perfectly plastic material condition which obeys Hooke's law to relate the stress and strains. Thus the material in FE analysis is controlled by the infinitesimal incremental stress and strain relationship. The strains and strain rates are decomposed into their elastic and plastic fraction during calculations. A drained Mohr–Coulomb sand under plane-strain condition

Fig. 8 Modelling of 90° screw nailed soil slope in Slope/W

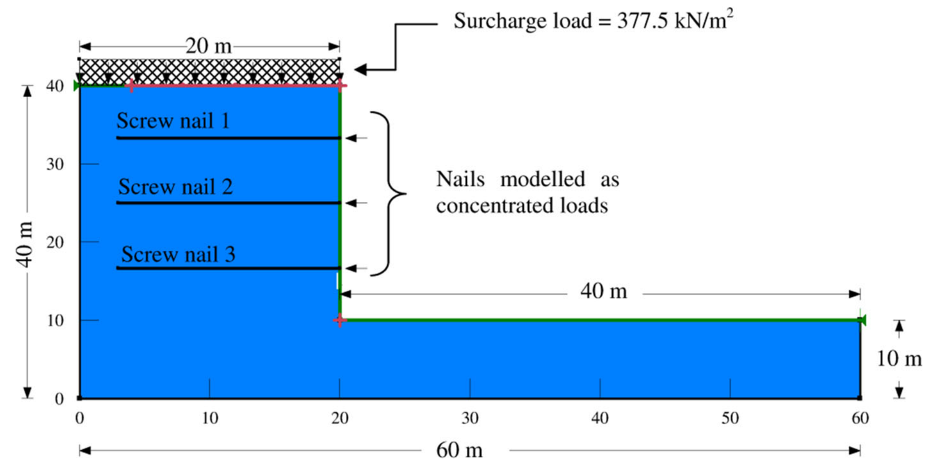

Table 6 Soil parameters used in Plaxis 2D

Parameters	Values
Modulus of elasticity (E_{soil})	50,000 kN/m^2
Poisson's ratio (υ)	0.33
Bulk unit weight (γ)	16.5 kN/m^3
Saturated unit weight (γ_{sat})	18.58 kN/m^3
Dilation angle ($\Psi°$)	0.79°

can best be used to simulate the actual soil conditions of model testing with γ_d, c and $\phi°$ values taken from Table 1. The other parameters used for soil modelling are summarized in Table 6.

The simulation of nails is achieved by using plate element. It has been observed from literature [33, 39, 40] that flexural rigidity and axial stiffness are important parameters for soil–nail design. Babu and Singh [41] emphasis on using equivalent modulus of elasticity (E_{eq}), equivalent axial stiffness (EA), equivalent bending stiffness (EI) and equivalent plate diameter (d_{eq}) for correct simulation of the soil nails, while using plate element.

The formulations by Babu and Singh [41] have been modified for conversions as:

$$E_{eq} = E_{sn}\frac{A_{sn}}{A} + E_g\frac{A_{grout}}{A} \quad (6)$$

$$EA = \frac{E_{sn}}{S_h}\frac{\Pi}{4}d_{sn}^2 \quad (7)$$

$$EI = \frac{E_{sn}}{S_h}\frac{\Pi}{64}d_{sn}^4 \quad (8)$$

$$d_{eq} = \sqrt{12\left(\frac{EI}{EA}\right)} \quad (9)$$

where, E_{sn} = Modulus of elasticity of screw nails (kN/m^2); A_{sn} = Area of screw nail (m^2); E_g = Modulus of elasticity of grout (kN/m^2); A_{grout} = Grout area (m^2); d_{sn} = diameter of screw nail used (m); S_h = Horizontal spacing of screw nails (m). Using Eqs. (6), (7), (8) and (9), the parameters corresponding to a circular cross-section of screw nail are modelled.

Plaxis 2D provides the opportunity to model proper soil–nail interaction by using an interface strength reduction factor (R_{inter}). This factor relates the soil shear strength parameters (c and ϕ) with interface strength as:

$$R_{inter} = \frac{\tan \emptyset_{interface}}{\tan \emptyset_{soil}} = \frac{\tan \delta}{\tan \emptyset} \quad (10)$$

$$R_{inter} = \frac{c_{interface}}{c_{soil}} \quad (11)$$

By substituting the value of $\tan\,\delta = 0.740$ and $\tan\,\phi = 0.596$ as determined from direct shear test in Eqs. (10) and (11), R_{inter} comes out to be 1.24. However, Plaxis 2D accepts a maximum value of $R_{inter} = 1$ for rough surfaces, which is also used for the present study. Further, an interface of virtual thickness factor (t_f) equal to height of thread of 0.15 is taken on either of modelled screw nail. During 2D mesh generation, this virtual thickness factor is multiplied by element thickness to create the desired interface. The parameters used for screw nail modelling are given in Table 7.

A surcharge load of 512.5 and 377.5 kN/m^2 is applied at slope crest of 45° and 90° respectively. The generated mesh is refined at interfaces and line of load application. The complete numerical model for 90° slopes is shown in Fig. 9. The initial stresses generated in screw nailed soil slopes are considered by earth pressure at rest condition. For simulating the earth pressure, a K_0—procedure with $K_0 = (1 - \sin\phi)$ is used. With this the FE modelling of reinforced slopes is completed and ready for analysis.

The simulated models is also analysed by using Strength Reduction Method (SRM) or Phi-c reduction method for determining factor of safety. The shear strength parameters c and ϕ are reduced from their original values till failure of

Table 7 Screw nail modelling parameters in Plaxis 2D

Parameters	Values (units)
Modelling element	Plate
Modelling type	Elasto-plastic
Modulus of elasticity of screw nails (E_n)	200 GPa
Equivalent modulus of elasticity (E_{eq})	200 GPa
Equivalent axial stiffness (EA)	3.024×10^5 kN/m
Equivalent bending stiffness (EI)	4.838 kN (m^2/m)
Equivalent plate diameter (d_{eq})	13.85 mm
Interface strength reduction factor (R_{inter})	1
Interface of virtual thickness factor (t_f)	0.15

Table 8 Factor of safety by Slope/W

Slope angle	Nail type	Factor of safety
45°	Screw nail	2.43
90°	Screw nail	2.10

reinforced slopes is reached. To achieve that a total multiplier $\sum M_{sf}$ is used which controls the reduction of shear strength parameters. The value of $\sum M_{sf}$ at failure is the FOS for screw nailed soil slope under study.

Results from Numerical Modelling

Factor of Safety and Failure Surfaces from Slope/W

The screw nailed slopes of 45° and 90° are analysed by LEM and the obtained factor of safety (FOS) are given in Table 8. It can be observed that for both slope angles of 45° and 90°, a factor of safety greater than 2 is achieved. The 45° screw nailed slope has a factor of safety of 2.43, while a factor of safety of 2.10 is obtained for 90° slope reinforced with screw nails. These values of FOS are found to be much higher than the recommended FOS = 1.4 against failure [42], FOS = 1.5 for overall stability [35], FOS = 1.3 for global stability with screw nails [37].

As shown in Fig. 10a, the critical slip surface is found to pass through all screw nails. The contribution of screw nails for stability of reinforced soil mass is a function of its tensile strength and pullout resistance of screw nails beyond the failure surface. The length of screw nails behind slip surface represents the bond length or length of nail which provide the pullout resistance during slope failure. This constitutes the passive zone during slope failure. The active zone is the soil enclosed by shear failure surface. The stability of this zone leads to stability of slope. With the inclusion of screw nails in active zone, the normal force on the failure surface intersecting the screw nails is increased. This increase in normal force increases the overall resisting forces acting on failure surface. In addition to the mobilized cohesion along slip surface and soil weight normal component, an extra shear force due to horizontal component of pullout resistance is developed along slip surface. This additional resisting force induced due to screw nail introduction increases the stability of reinforced soil slope of 45°. The slip surface for 45° is

Fig. 9 Modelling of 90° screw nailed slope in Plaxis 2D

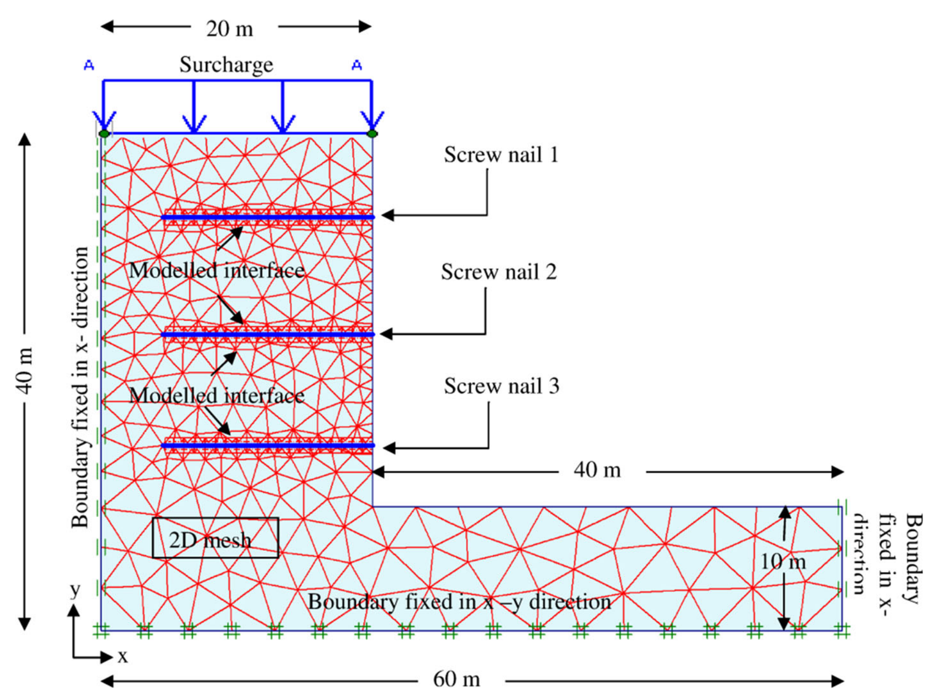

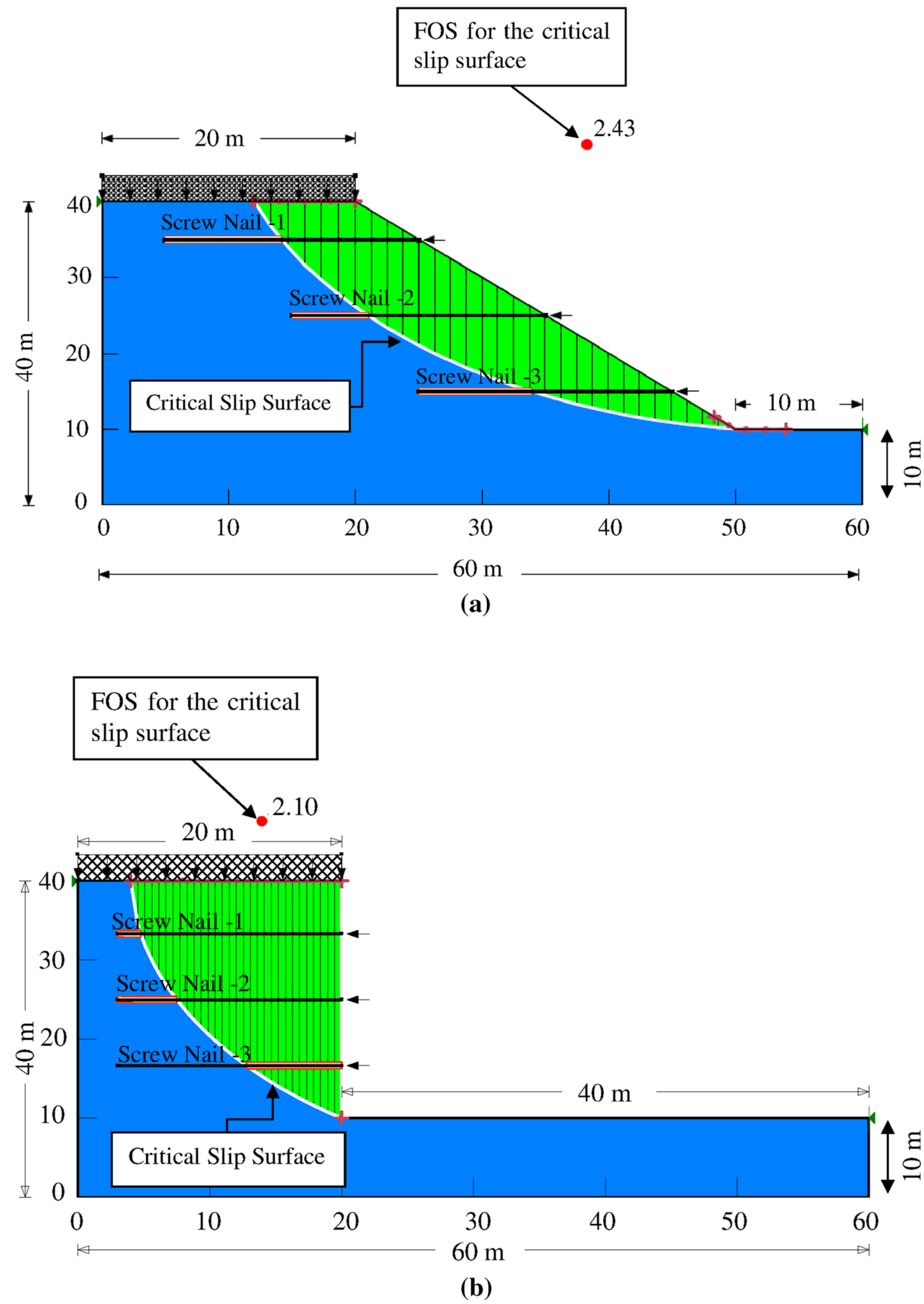

Fig. 10 **a** Factor of safety corresponding to critical slip surface for 45° screw nailed slope. **b** Factor of safety corresponding to critical slip surface for 90° screw nailed slope

found to pass through the toe of slope which is a mode of failure for global stability. The FOS of 2.43 > 1.3, suggests that screw nails in 45° soil slope provides global stability.

The global stability for 90° is also achieved by using screw nails, since the FOS of 2.10 > 1.3 is obtained. Moreover, failure slip surface for 90° is also found to pass through the toe of slope. It can be seen from Fig. 10b the failure surface intersects all the nails as in screw nailed slope of 45°. However, for screw nail-1 and screw nail-2, the pullout resistance of nails governs the load transfer mechanism during failure. For screw nail-3, the bond length required to mobilize the pullout of nails lies within the active zone of failure surface. This signifies that the load transfer mechanism is controlled by tensile strength of screw nails.

Factor of Safety and Failure Surfaces from Plaxis 2D

Table 9 shows the factor of safety obtained from SRM for 45° and 90° screw nailed soil slopes. It can be observed that a factor of safety >2 is achieved for both 45° and 90° slopes.

The 45° screw nailed slope has FOS = 2.37, whereas FOS = 2.06 is found for 90° screw nailed slope. A higher

Table 9 Factor of safety by Plaxis 2D

Slope angle	Nail type	Factor of safety
45°	Screw nail	2.37
90°	Screw nail	2.06

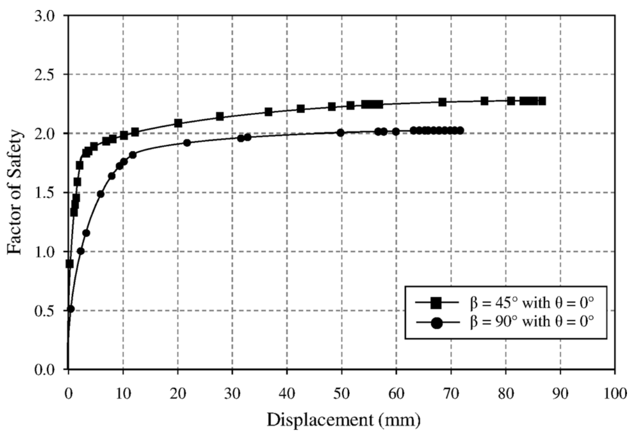

Fig. 11 Factor of safety from Plaxis 2D

FOS is found for slope angle (β) = 45° than $\beta = 90°$ as shown in Fig. 11, which is similar to FOS obtained from Slope/W. However, FOS from Slope/W are found to be on higher side as compared to FOS obtained from Plaxis 2D. The reason for this can be dependency of interslice weight and slice base force on assumed slip surface by Slope/W. Whereas FEM based Plaxis 2D locates the potential slip surface in zones of excessive strains and calculates the FOS [43]. This difference in slip surface determination and corresponding FOS can be accounted for higher FOS by Slope/W than Plaxis 2D.

The slip surfaces as obtained from Plaxis 2D given in Fig. 12a, b clearly shows that at failure the plastic strains are developed within the reinforced slopes. The location of plastic stain points yields the potential slip surface and corresponding FOS values. As shown in Fig. 12a, 45° screw nailed slope has a slip surface intersecting nails at all locations. The slip surface can also be seen passing through the slope toe. The critical slip surface corresponding to maximum displacement clearly divides the soil mass into active and passive zones. The length of screw nails in active soil zone is sufficient enough to arrest the slip occurring between soil–soil interface. Due to rough surface of screw nails, the interface friction increases between soil and nail. This increased interface friction is mobilized as the soil mass fails under surcharge load. As the soil deformation increases, large strains are generated in the vicinity of screw nails, which enhance the reinforcing action of nails and hence the stability of reinforces slope. A similar slip surface is also obtained from Slope/W analysis.

As shown in Fig. 12b, the slip surface for 90° screw nailed slope is also found passing through the slope toe. The slip surface passes through the nail and thus utilizes its pullout resistance towards horizontal deformation. Figure 12b also suggests that the length of top and middle screw nail is completely utilized to mobilize the pullout resistance of screw nails. However, for bottom screw nail, a smaller length of nail is sufficient for providing the shear resistance against failure. The failure slip surface from Plaxis 2D is found in good agreement with Slope/W analysis.

Deformation of Screw Nailed Slopes from Plaxis 2D

In order to obtain the slope deformation of reinforced slopes of 45° and 90°, an elastic–plastic analysis is carried out by Plaxis 2D. The deformed geometry of 45° reinforced slope can be seen in Fig. 13a. It is evident that under surcharge load the settlement of crest has taken place. This settlement of slope crest can be accounted for the fact that soil undergoes compression as surcharge is gradually increased. This effect of increasing surcharge is transferred to the top screw nail. In addition to the overburden, an additional surcharge is now being beared by the top nail. Simultaneously, the strain values are increasing due to increase in stress. This leads to the formation of plastic strain zones in reinforced slopes. If these plastic strain zones lie within the reinforced slope mass, the deformations are small and within limit. These deformation characteristics are a necessary for assessing the serviceability of screw nailed soil slope system. The load at failure for 45° reinforced slope is found to be 37.91 kN with a slope displacement of 84.74 mm.

It can also be investigated from Fig. 13a, that due to development of plastic strain, the slope geometry has changed at slope face. The deformation of slope face together with displaced screw nails signify that both the axial stiffness and bending stiffness of screw nails have been mobilized. The bending of screw nail can be due to the overburden acting above each nail. The displacement of slope mobilizes the interface shearing between screw nail and soil. As more and more soil goes into plastic deformation, an increase in interface friction takes place. This increased shearing between soil and screw nails develops tensile forces in the nails. This developed tension in screw nails along with increased surface roughness regulates the slope movement to a minimum.

For 90° screw nailed slope, a slope displacement of 44.24 mm is reached as the slope fails at load of 27.37 kN. It can be clearly seen from Fig. 13b that in a 90° vertical cut, small deformation is observed near the slope toe.

As the height of wall increases, the deformations increase towards the crest. Analogous to crest settlement in

Fig. 12 **a** Failure slip surfaces for 45° screw nailed slope. **b** Failure slip surfaces for 90° screw nailed slope

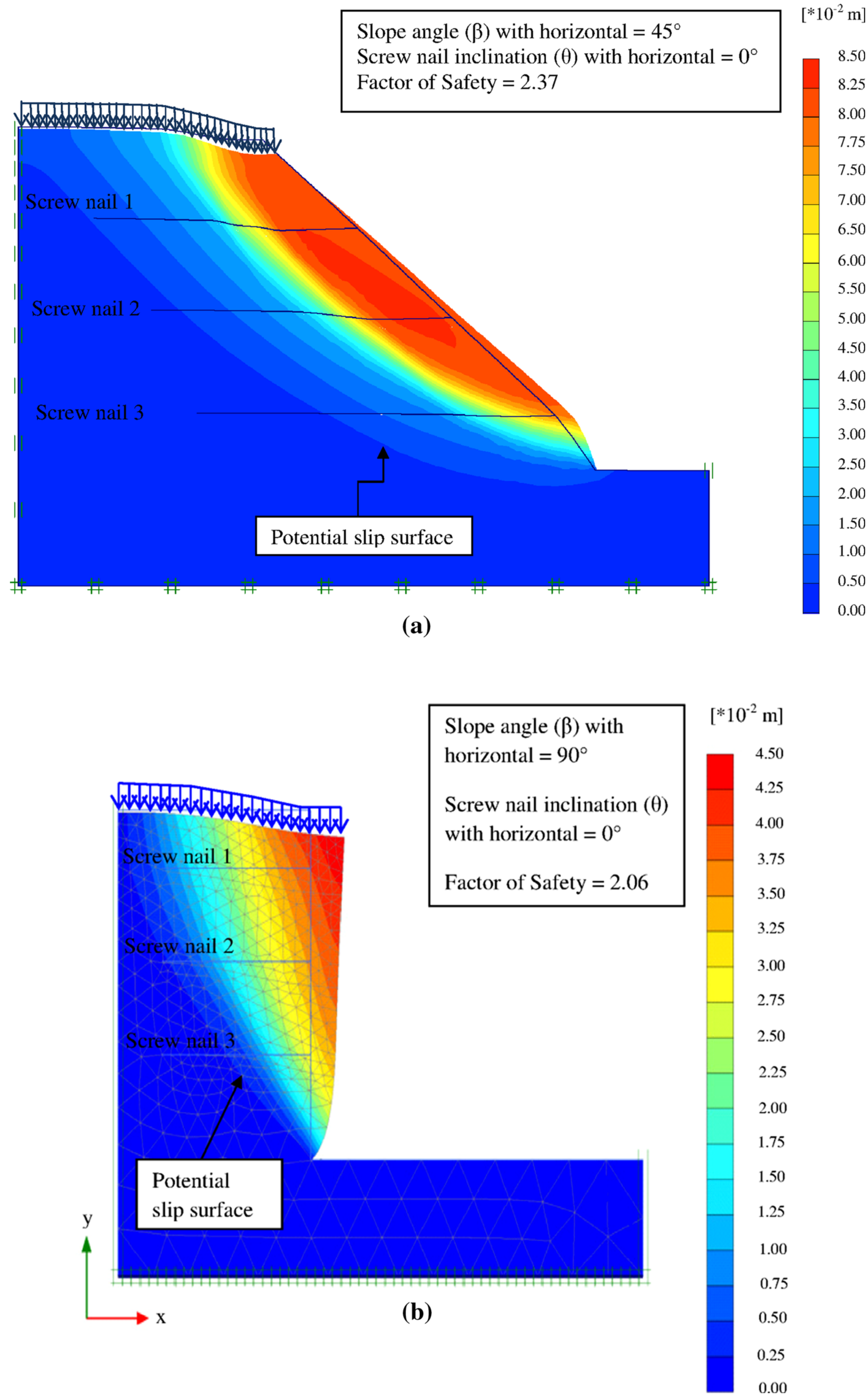

45° reinforced slope, the crest of 90° screw nailed slope is also found to settle. This settlement can be attributed to soil compression under surcharge load. It can also be said from deformation pattern obtained for 90° that large plastic strain are developed at slope face near the crest. This also means that screw nails near the top of slope plays more part in slope stabilization of steep cuts as compared to bottom screw nails. This is evident from the dislocation of top and middle nails as observed from their initial level, which is greater than the displacement of bottom screw nail from its

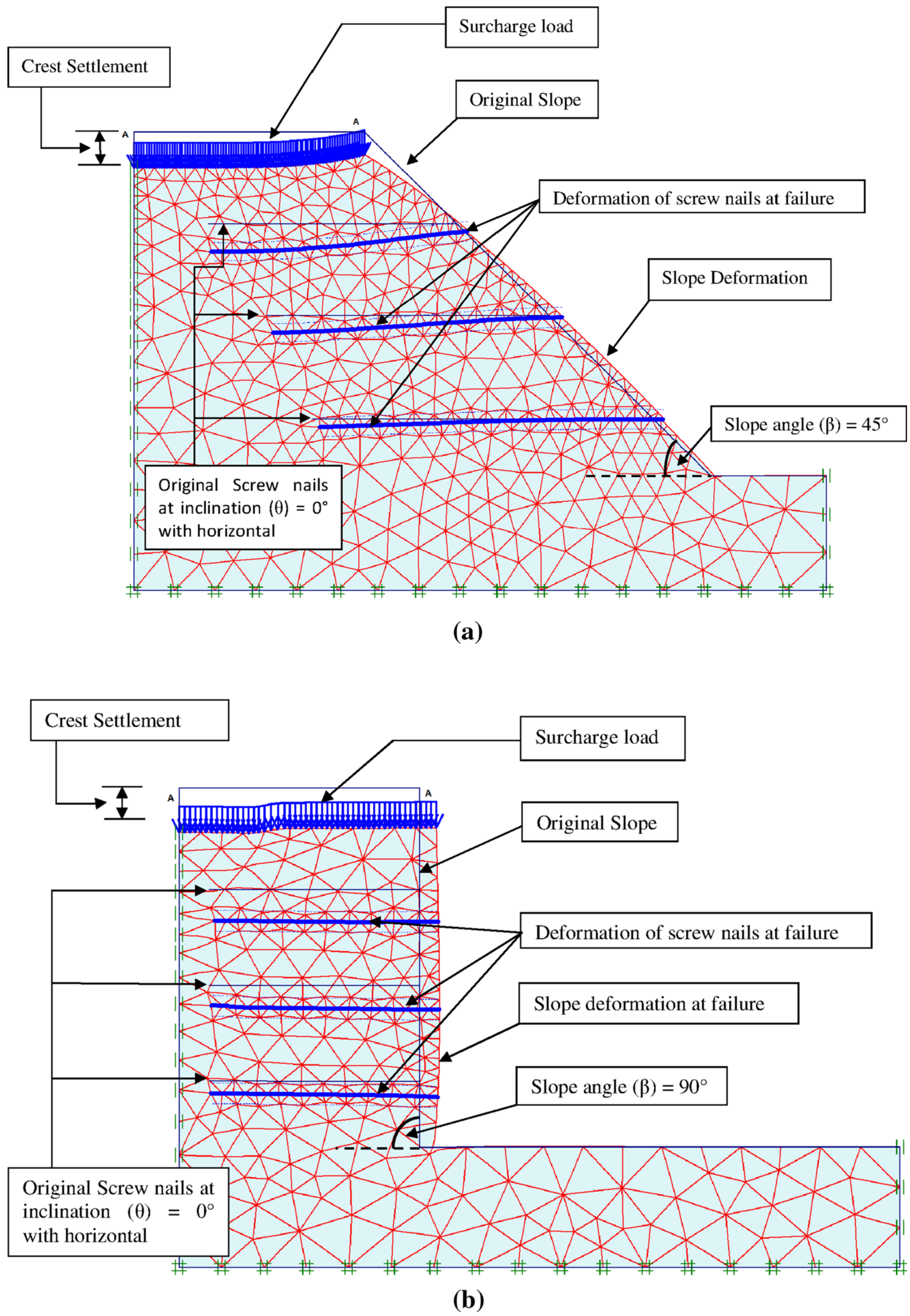

Fig. 13 **a** Deformation at failure load for 45° screw nailed slope. **b** Failure slip surfaces for 90° screw nailed slope

Table 10 Failure load–displacement results from Plaxis 2D

Slope angle	Nail type	Failure load (kN)	Displacement (mm)
45°	Screw nail	37.91	84.74
90°	Screw nail	27.37	44.24

original position. Also negligible bending of nails can be observed for all three screw nail locations. This signifies that for 90° reinforced slope, axial stiffness of screw nails is mobilized than bending stiffness. The load–displacement results from Plaxis 2D is summarized in Table 10.

Volumetric Deformation of Screw Nailed Slopes from Plaxis 2D

The volumetric deformation of reinforced slopes can be studied from percentage volumetric strains as obtained from Plaxis 2D analysis. Percentage volumetric strain is change in strains in x, y and z directions respectively. It also corresponds to change in reinforced slope volume to original slope volume under failure load. As shown in Fig. 14a, b, volumetric strains for 45° slope is 9.12%, whereas 2.85% is observed for 90° screw nailed slope.

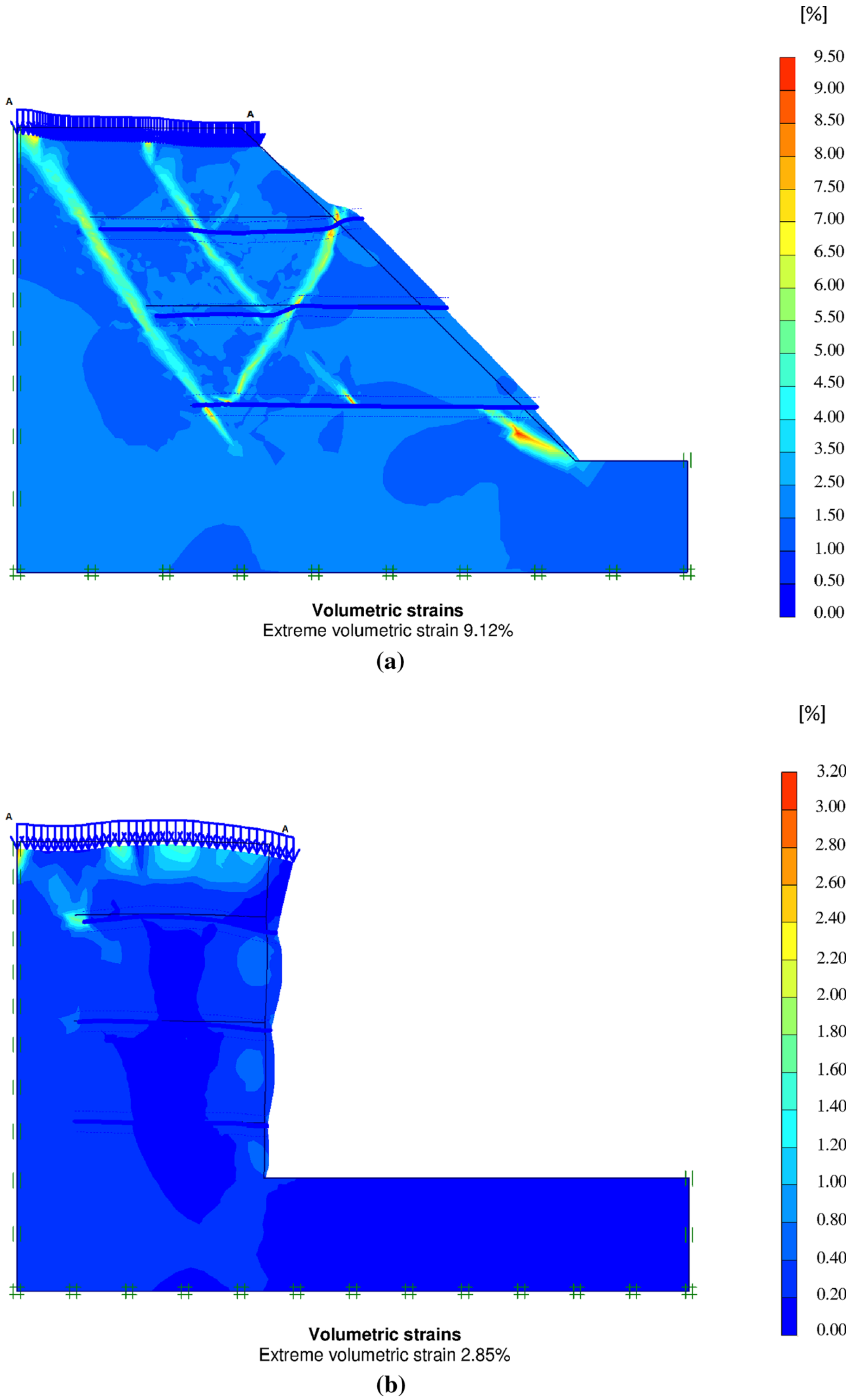

Fig. 14 **a** Volumetric strains developed in 45° screw nailed slope. **b** Volumetric strains developed in 90° screw nailed slope

From volumetric strain figures, it is evident that large volume changes occur in 45° slope as compared to 90° slopes. Moreover, this can be justified by the fact that 45° reinforced slope depicts a greater displacement of 84.74 mm in contrast to 90° reinforced slope where displacement of only 44.24 mm is observed. Figure 14a, b further suggests that more volume changes occur at slope crest, screw nail ends and slope toe for 45° slope. However, for 90° screw nailed slope, the major volume changes are concentrated at the crest. This also can be a reason for greater displacements at slope crest than slope toe for 90° slope. From Fig. 14b, it can be seen that large volume

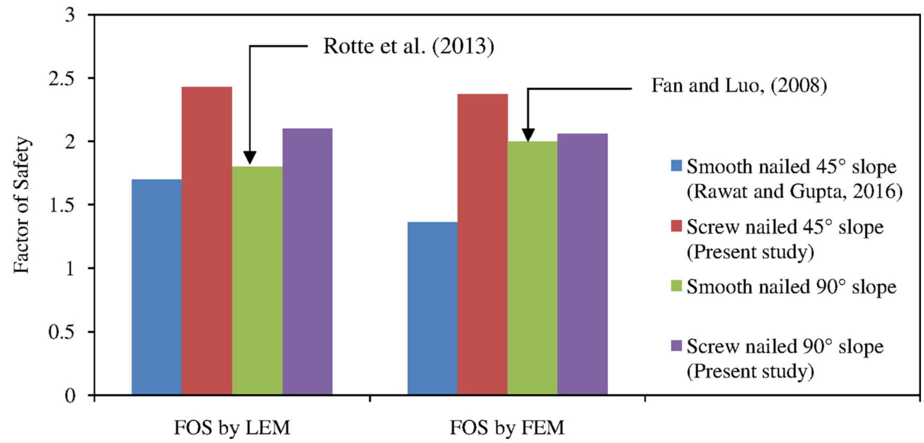

Fig. 15 Comparison of FOS between screw nailed slopes and smooth nailed slopes

change occurs between top and middle screw nails than middle and bottom screw nails. Moreover, a small volume change is observed below the bottom screw nail. The increase in displacement with wall height can be attributed to these variations in volumetric deformation.

Validation of Model Testing Results by Numerical Modelling Results

Failure Slip Surface

As observed from Figs. 5b and 6b, model testing of screw nailed soil slopes of 45° and 90° shows a slip surface originating from the crest and propagating towards the slope face terminating above the toe under the surcharge load. Such failure surface has also been reported by Schlosser [44] for soil nailed structures using limit equilibrium method. Gassler and Gudehus [45] has also identified bi-planar and circular slip surface in small model tests on slopes. Local cracking is also observed near the toe and around the slip surface. For 90° screw nailed slope, the slip surface is rather complex and highly irregular. The slip surface is closer to slope face which causes it to deform significantly. The slip surface generated by Slope/W as shown in Fig. 10a, b depicts that for both 45° and 90°, the slip surface begins under surcharge load at slope crest and end at slope toe. The shape of slip surface can be treated as circular. However, Fig. 10b depicts critical surface for reinforced slope of 90° with minimum factor of safety of safety of 2.10. The slip surface is very unlikely for slope of 90° as it has also been observed from model testing. The reason for this clearly brings out a limitation of limit equilibrium method in evaluating the stability of nailed slopes. The limit equilibrium method (SLOPE/W) does not incorporate the deformation of slope during failure. The critical slip surface is obtained by error and trial method such that a minimum factor of safety is obtained for which force and moment equilibrium are found to converge. To overcome this limitation, critical slip surface and corresponding factor of safety are also validated by finite element method (PLAXIS 2D) which incorporates the load–deformation of slopes at failure. The slip surfaces obtained from Plaxis 2D (Figs. 12a, b) are similar to failure surfaces from Slope/W such that the rupture surface starts at slope crest and terminates at toe with variation in shape of slip surface. Plaxis 2D yields non-circular failure surfaces for both 45° and 90° screw nailed slope. Moreover, finite element analysis of 90° slope depicts that rupture surface passes through the toe and meets the crest at right angles. For this reason, it has been treated as a non-circular slip surface.

The origin of slip surface developing from slope crest is common for model testing and numerical modelling. However, numerical modelling of reinforced slopes suggests that failure envelop should terminate at toe of slope. On the contrary, model testing shows that failure surfaces terminate above slope toe for both slopes. This variation in slip surface location can be due to remoulding of soil around screw nails at the time of installation. The installation torque remoulds the in-situ soil and can alter its shear strength properties. Due to this variation in 'c' and 'ϕ' around screw nails with respect to rest of the soil slope brings about a change in failure surface shape. Incase of numerical modelling, the installation torque is neglected both in Slope/W and Plaxis 2D, hence soil properties are homogeneous throughout the slope body. Thus, defined shear strength parameters of soil are mobilized only, which are different from shear parameters mobilized during testing. This accounts for variation in shape of failure surface obtained from model tests and numerical modelling.

The factor of safety obtained from numerical analysis are compared with FOS against failure found from literature on same reinforced slope of 45° and 90° with smooth nails. As shown in Fig. 15, it can be seen that screw nails gives a better slope stability than smooth nails for same

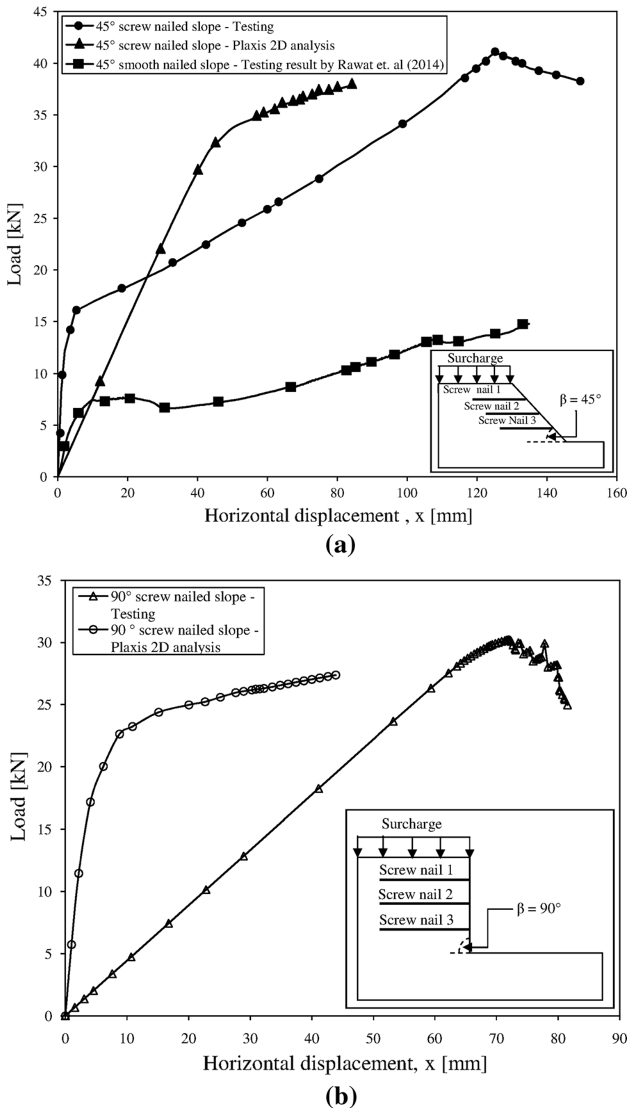

Fig. 16 **a** Load–displacement comparison between model testing, FEM and with smooth nails for 45° slopes. **b** Load–displacement comparison between model testing, FEM and with smooth nails for 90° slope

slope angles. For numerical modelling of screw nailed slopes both by LEM and FEM, FOS > 2 is obtained, whereas FOS < 2 is reported for stability of slope using smooth nails. This increase in FOS for screw nailed slopes can be accounted for the increased interface friction provided by surface roughness of screw nails in comparison to smooth nails.

Load-Deformation Characteristics

From model testing and Plaxis 2D analysis as shown in Fig. 16a, b, it can be deduced that as the surcharge load is increasing on slope crest, the slope is undergoing a horizontal displacement. However, larger displacement and higher failure loads are achieved from model testing in comparison to FEM analysis. The reason for this variation can be difference in actual and modelled boundary conditions of reinforced slopes. In model testing, the increasing surcharge load causes compression of reinforced slope model, which is restricted in all three directions i.e. length, width and height by Perspex sheets. Due to the flexible Perspex sheet boundaries, small lateral expansion of screw nailed slopes might have occurred during failure. However, no significant physical changes were observed during testing. However, smaller displacement of numerical model can be due simulation in plain strain 2D environment. Moreover, higher failure load during model testing can be attributed to large horizontal movements, which mobilize greater interface friction and increase the slope bearing capacity. For numerical modelling, theoretical pullout value is used for simulating screw nails which might vary from actual pullout resistance developed by screw nails. The variation in analytical pullout value in comparison to pullout from testing can be due to the fact that pullout in screw nails is different from that in a conventional smooth nail. The threads of nail enhance the soil around its tip which increases the effective screw nail diameter. This makes the failure surface shift deep into the soil during pullout [3].

In the absence of literature regarding pullout of screw nails as used in present work, it leaves an opportunity for other researchers to experimentally determine the pullout resistance of these screw nails. Hence, it can be said that if numerical modelling is carried out in 3D environment with actual pullout values for screw nails, a much closer agreement in load–deformation can be reached between model testing and numerical modelling.

A comparative study between screw nailed soil slopes of present study and smooth nailed soil slopes as done by researchers in the past reveals that screw nails increase the load carrying capacity and decreases horizontal movement of slopes under gradual increase surcharge load. As shown in Fig. 16a, model testing carried out by Rawat et al. [20] on reinforced slopes with smooth nails for 45° slopes has a maximum load carrying capacity of 14.79 kN with 134.85 mm slope movement. By using screw nails for the same slope angle, the bearing capacity has increased to 41 kN and displacements are minimized to 125 mm. An increase of 177% in load carrying capacity and decrease of about 7% is attained in slope displacement. However, the vast increase in load carrying capacity can also be due to a greater cohesion value of soil used in present study than by Rawat et al. [20].

Volumetric Deformations

From Fig. 17, it can be seen that volumetric deformations of 11 and 5.6% are obtained from model testing for 45° and

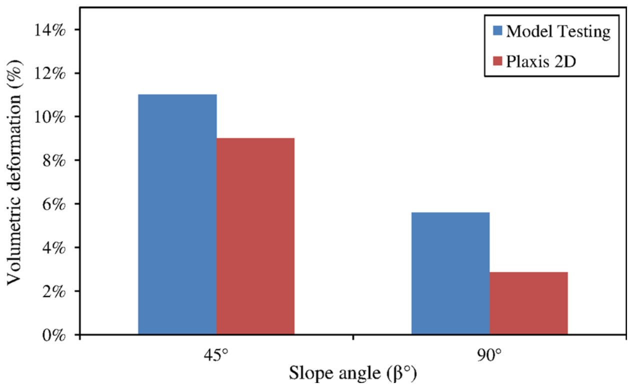

Fig. 17 Volumetric deformation comparison between model testing and Plaxis 2D

90° respectively. However, Plaxis 2D analysis predict smaller volumetric deformations of 9% for 45° screw nailed slope and 2.85% for 90° slope. It can be seen that model testing shows an increase of 2% for 45°slope and 2.75% for 90° slope. The difference in volumetric deformation determination from model testing and Plaxis 2D can be due to difference in boundary conditions and screw nail installation effect (installation torque) on soil parameters.

Conclusions

The present study deals with testing and modelling of 45° and 90° reinforced soil slopes with screw nails at an inclination of 0° with horizontal. Based on the results obtained from testing and analysis by Slope/W and Plaxis 2D, the following conclusions can be made:

1. The screw nails used in present work produces a greater interface friction between soil–nail interface than conventional nails. This is due to the threaded/rough surface which increases the soil–nail interaction. This increased interaction affect in the soil around screw nail to a larger distance, thereby increasing the effective diameter of nail contributing in screw nail pullout resistance. The failure surface shifts deep into the soil and an overall increased pullout resistance is achieved.
2. The factor of safety for screw nailed soil slopes of 45° and 90° are found to be greater than 2. This satisfies all the recommended values of FOS reported by different agencies working on soil–nail system. Moreover, the FOS values for screw nailed soil slopes are greater than those achieved by researchers in past for smooth soil nails. Both Slope/W and Plaxis 2D analysis gives FOS > 2 for screw nailed slopes whereas smooth nailed soil slopes have yielded FOS < 2. This concludes that screw nails provides global stability and are effective in slope stabilization.
3. The failure surface from model testing and numerical modelling are found to differ. This variation can be accounted to the change in soil properties due to installation torque applied on screw nails. This installation torque remoulds the in-situ soil and alters its shear parameters. Numerical modelling does not simulate the installation of nail, hence no change in shear parameters of soil are taken into account during the analysis. However, both Slope/W and Plaxis 2D gives a similar slip surface pattern. Hence it can be concluded that installation effects should be considered for a screw nail system.
4. The deformation of slopes in model testing is found in good agreement to numerical modelling deformations with slight variations for both 45° and 90° slopes. The slope displacement has been reduced by 7% in comparison to displacement of slopes reinforced by smooth nails for 45° slope with an increase in load bearing capacity of slope. So, it can be concluded that screw nails perform satisfactorily in slope stabilization based on load–deformation of screw nailed slopes.
5. A small variation of about 2% in volumetric deformations is found between model testing and numerical modelling of both slopes. However, locations of significant volumetric deformations are found to be similar both from testing and modelling. The small percentage of volumetric deformation achieved for both slope further reflects the efficiency of screw nails in slope stabilization. It can also be inferred from the results of volumetric deformation that screw nails are more effective for steep slope ($\beta = 90°$).
6. During installations of screw nails in soil model, negligible spoils are found to be produced. Moreover, easy installation is observed by simply applying torque on nail head without significant disturbance to the entire soil mass as done during driving of conventional soil nails. No noises are produced during screw nail installations. With these installation privileges and parameters discussed above, it can be concluded that screw nails have certain advantages over conventional nails both in terms of performance, serviceability and ease of installation.

References

1. Luo SQ, Tan SA, Yong KY (2000) Pull-out resistance mechanism of a soil nail reinforcement in dilative soils. Soil Found Jpn Geotech Soc 40(1):47–56

2. Zhou WH, Yin JH, Hong CY (2011) Finite element modelling of pullout testing on a soil nail in a pullout box under different overburden and grouting pressures. Can Geotech J 48(4):557–567
3. Tokhi H (2016) A study of new screw soil nail. Dissertation, RMIT University, Melbourne
4. Prashant A, Mukherjee M (2010) Soil nailing for stabilization of steep slopes near railway tracks. Research Design and Standard Organisation, Lucknow
5. Shaw-Shong L (2005) Soil nailing for slope strengthening. Geotechnical Engineering Gue & Partners Sdn Bhd, Kuala Lumpur
6. Wang Z, Richwien W (2002) A study of soil-reinforcement interface friction. J Geotech Geoenviron Eng 128(1):92–94
7. Gosavi M, Saran S, Mittal S (2008) Evaluation of apparent coefficient of friction between soil and nails. In: Proceedings of the 12th international conference of the international association for computer methods and advances in geomechanics (IACMAG), Goa, pp 1346–1354
8. Cartier G, Gigan JP (1983) Experiments and observations on soil nailing structures. In: Paper presented at the 8th European conference on soil mechanics and foundation engineering, Helsinki, Finland
9. Milligan GWE, Tei K (1998) The pull-out resistance of model soil nails. Soils Found 38(2):179–190
10. Franzén G (1998) Soil nailing. A laboratory and field study of pullout capacity. Doctoral dissertation, Chalmers University of Technology
11. Junaideen SM, Tham LG, Law KT, Lee CF, Yue ZQ (2004) Laboratory study of soil–nail interaction in loose, completely decomposed granite. Can Geotech J 41(2):274–286
12. Pradhan B (2003) Study of the pull-out behaviour of soil nails in completely decomposed granite fill. M.Phil., University of Hong Kong
13. Su L, Chan T, Yin J, Shiu Y, Chiu S (2008) Influence of overburden pressure on soil–nail pullout resistance in a compacted fill. J Geotech Geoenviron Eng 134(9):1339–1347
14. Wu JY, Zhang ZM (2009) Evaluations of pullout resistance of grouted soil nails. In: Ge L, Liu J, Ni JC, Yi He Z (eds) Slope stability, retaining walls, and foundations; Selected papers from the 2009 GeoHunan internatinal conference. American Society of Civil Engineers (ASCE), Reston, USA, pp 108–114
15. Hong CY, Yin JH, Pei HF (2013) Comparative study on pullout behaviour of pressure grouted soil nails from field and laboratory tests. J Cent South Univ 20:2285–2292
16. Chu LM, Yin JH (2005) Comparison of interface shear strength of soil nails measured by both direct shear box tests and pullout tests. J Geotech Geoenviron Eng 131(9):1097–1107
17. Kim D, Juran I, Nasimov R, Drabkin S (1995) Model study on the failure mechanism of soil-nailed structure under surcharge loading. Geotech Test J 18(4):421–430
18. Kodaka T, Akira A, Pokharel G (1995) Model tests and theoretical analysis of reinforced soil slopes with facing panels. Soils Found Jpn Soc Soil Mech Found Eng 35(1):133–145
19. Gosavi M, Saran S, Mittal S (2009) Model tests for validation of analysis of nailed cuts. Indian Geotech J 39(1):96–116
20. Rawat S, Zodinpuii R, Manna B, Sharma KG (2014) Investigation on failure mechanism of nailed soil slopes under surcharge loading: testing and analysis. Geomech Geoeng 9(1):18–35
21. Rawat S, Gupta AK (2016) An experimental and analytical study of slope stability by soil nailing. Electron J Geotech Eng 21(17):5577–5597
22. Zhang M, Song E, Chen Z (1999) Ground movement analysis of soil nailing construction by three-dimensional (3-D) finite element modeling (FEM). Comput Geotech 25(4):191–204
23. Srinivasa Murthy BR, Sivakumar Babu GL, Srinivas A (2002) Analysis of prototype soil-nailed retaining wall. Proc Inst Civ Eng Ground Improv 6(3):129–136
24. Fan CC, Luo JH (2008) Numerical study on the optimum layout of soil nailed slopes. Comput Geotech 35(4):585–599
25. Rotte V, Viswanadham B, Chourasia D (2011) Influence of slope geometry and nail parameters on the stability of soil-nailed slopes. Int J Geotech Eng 5(3):267–281
26. Chan CM, Raman MHA (2017) Screw-in soil nail for slope reinforcement against slip failure: a lab-based model study. Int J 12(29):148–155
27. Bruce DA, Jewell RA (1986) Soil nailing: application and practice-part 1. Ground Eng 19(8):10–15
28. Gosavi MS (2006) Behaviour of nailed open cuts. Doctoral dissertation, Indian Institute of Technology, Roorkee
29. Zhang G, Cao J, Wang L (2014) Failure behavior and mechanism of slopes reinforced using soil nail wall under various loading conditions. Soils Found 54(6):1175–1187
30. Plumelle C, Schlosser F (1990) A French national research project on soil nailing: CLOUTERRE. In: Performance of reinforced soil structures proceedings of international reinforced soil conference, Glassgow, pp 219–223
31. Byrne RJ, Cotton D, Porterfield J, Wolschlag C, Ueblacker G (1996) Manual for design and construction monitoring of soil nail walls. No. FHWA-SA-96-069
32. Gosavi M, Saran S, Mittal S (2009) Pseudo-static analysis of soil nailed excavations. Geotech Geol Eng 27(4):571–583
33. Tei K (1993) A study of soil nailing in sand. Doctoral dissertation, Magdalen College, University of Oxford
34. Kulhawy FH, Peterson MS (1979) Behavior of sand-concrete interfaces. In: Proceedings of 6th Pan-American conference on soil mechanics and foundation engineering vol. 7, pp 225–236
35. FHWA (2003) Geotechnical engineering circular No. 7—soil nail walls. Report FHWA0-IF-03–017. US Department of Transportation Federal Highway Administration, Washington DC
36. SLOPE/W (2001) A software package for slope stability analysis, Ver. 5. Geo-Slope International, Calgary, Alta
37. Hubble Power Systems Inc (2015) Screw nailing retention earth structures. Design manual, CHANCE USA
38. Brinkgreve RBJ (ed) (2002) Plaxis: finite element code for soil and rock analyses: 2D-Version 8. User's Guide Balkema
39. Shiu YK, Chang GWK (2006) Effects of inclination, length pattern and bending stiffness of soil nails on behavior of nailed structures. GEO Report No.197 Geotchnical Engineering Office, Hong Kong
40. Chmoulian AY (2015) Effect of axial stiffness on soil nail forces. Proc Inst Civ Eng Geotech Eng 168(1):42–52
41. Babu GS, Singh VP (2009) Simulation of soil nail structures using PLAXIS 2D. Plaxis Bull 25:16–21
42. Geoguide 7 (2008) Guide to soil nail design and construction. Geotechnical Engineering Office, Civil Engineering and Development Department, The Government of the Hong Kong Special Administrative Region
43. Rawat S, Gupta AK (2016) Analysis of a nailed soil slope using limit equilibrium and finite element methods. Int J Geosynth Ground Eng 2(4):34
44. Schlosser F (1982) Behaviour and design of soil nailing. In: Symposium on recent developments in ground improvement techniques, Bangkok, pp 399–413
45. Gassler G, Gudehus G (1981) Soil nailing—some aspects of new technique. In: Proceedings of tenth ICSMFE, Stockholm, Balkema, pp 943–962